Heliyon 10 (2024) e29374

Contents lists available at ScienceDirect

Heliyon

journal homepage: www.cell.com/heliyon

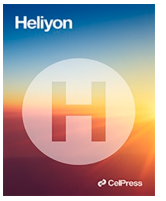

Research article

Deciphering the role of non-coding RNAs involved in sorafenib resistance

FanJing Jing [a], YunYan Shi [a], Dong Jiang [b], Xiao Li [a], JiaLin Sun [a], XiaoLei Zhang [a], Qie Guo [a,*]

[a] *Department of Clinical Pharmacy, The Affiliated Hospital of Qingdao University, Qingdao, Shandong, 266003, PR China*
[b] *Navy Qingdao Special Service Rehabilitation Center, 266743, Qingdao, Shandong, 266003, PR China*

ARTICLE INFO

Keywords:
Hepatocellular carcinoma
Sorafenib
Non-coding RNAs
Long non-coding RNAs
Circular RNAs
MicroRNAs

ABSTRACT

Sorafenib is an important treatment strategy for advanced hepatocellular carcinoma (HCC). Unfortunately, drug resistance has become a major obstacle in sorafenib application. In this study, whole transcriptome sequencing (WTS) was conducted to compare the paired differences between non-coding RNAs (ncRNAs), including long non-coding RNAs (lncRNAs), circular RNAs (circRNAs), microRNAs (miRNAs), and mRNAs, in sorafenib-resistant and parental cells. The overlap of differentially expressed ncRNAs (DENs) between the SMMC7721/S and Huh7/S cells and their parental cells was determined. 2 upregulated and 3 downregulated lncRNAs, 2 upregulated and 1 downregulated circRNAs, as well as 10 upregulated and 2 downregulated miRNAs, in both SMMC7721/S and Huh7/S cells, attracted more attention. The target genes of these DENs were then identified as the overlaps between the differentially expressed mRNAs achieved using the WTS analysis and the predicted genes of DENs obtained using the "co-localization" or "co-expression," *miRanda,* and *RNAhybrid* analysis. Consequently, the potential regulatory network between overlapping DENs and their target genes in both SMMC7721/S and Huh7/S cells was explored. The "lncRNA-miRNA-mRNA" and "circRNA-miRNA-mRNA" networks were constructed based on the competitive endogenous RNA (ceRNA) theory using the Cytoscape software. In particular, lncRNA MED17-203-miRNA (miR-193a-5p, miR-197-3p, miR-27a-5p, miR-320b, miR-767-3p, miR-767-5p, miR-92a-3p, let-7c-5p)-mRNA," "circ_0002874-miR-27a-5p-mRNA" and "circ_0078607-miR-320b-mRNA" networks were first introduced in sorafenib-resistant HCC. Furthermore, these networks were most probably connected to the process of metabolic reprogramming, where the activation of the PPAR, HIF-1, Hippo, and TGF-β signaling pathways is governed. Alternatively, the network "circ_0002874-miR-27a-5p-mRNA" was also involved in the regulation of the activation of TGF-β signaling pathways, thus advancing Epithelial-mesenchymal transition (EMT). These findings provide a theoretical basis for exploring the mechanisms underlying sorafenib resistance mediated by metabolic reprogramming and EMT in HCC.

1. Introduction

Hepatocellular carcinoma (HCC) is the fourth leading cause of cancer-related deaths worldwide [1]. Most patients are diagnosed

* Corresponding author.
E-mail address: guoqie822a@qdu.edu.cn (Q. Guo).

https://doi.org/10.1016/j.heliyon.2024.e29374
Received 8 December 2023; Received in revised form 2 April 2024; Accepted 7 April 2024
Available online 13 April 2024

during clinically advanced stages due to the early symptoms of hiding [2]. Sorafenib, a multiple-kinase inhibitor, is the first-line drug for treating advanced HCC [3]. However, drug resistance is a major obstacle for many patients with advanced HCC, leading to an unsatisfactory survival rate [4]. Elucidating the mechanism of sorafenib resistance and identifying targets for reversing drug resistance have, therefore, become top priorities.

Recently, non-coding RNAs (ncRNAs), including long non-coding RNAs (lncRNAs), circular RNAs (circRNAs), and microRNAs (miRNAs), have been received increasing attentions. They have been found to transcriptionally and post-transcriptionally regulate vital processes in the progression of complex diseases, especially cancers [5]. In particular, lncRNAs are RNA molecules with lengths greater than 200 nt, and they generally do not encode proteins. LncRNAs have been ignored as useless transcripts for the longest time but have recently been found to play essential reoles in the pathogenesis of numerous diseases, such as cancer and immune deficiency disorders [6]. As newly discovered epigenetic RNA, lncRNAs also play vital roles in oncogenesis and tumor progression in HCC [7]. CircRNAs with a length of over 200 nt are mainly produced by precursor mRNA (pre-mRNA) through variable splicing processing; the 5'and 3′ ends covalently combine to form a closed structure, widely present in animals and plants. Its unique circular structure allows it to evade the degradation by RNA enzymes and enhances internal stability [8]. CircRNAs have been proven to be widely distributed in cancer progression and are novel biomarkers and therapeutic targets for HCC [9,10]. MiRNAs represent a class of small endogenous ncRNAs located at fragile sites and breakpoints associated with tumors [11], where they are involved in most biological processes by imposing regulation on the expression of target genes [12]. MiRNAs have emerged as putative targets for the diagnosis, clinical treatment and prognostic evaluation of HCC [13].

LncRNAs or circRNAs can serve as miRNA "sponges" by targeting the common miRNA response elements to construct an RNAse-induced silencing complex, thus regulating the expression of target mRNA. This global mechanism, known as competitive endogenous RNA (ceRNA), was first described in 2011 [14]. In recent years, the understanding of the mechanisms of ncRNAs in the development of drug resistance in tumor cells has continuously improved on a continued basis, in which a ceRNA-based regulatory mechanism is involved [15]. However, exploration of novel ncRNAs and a clear consensus on the detailed mechanisms involved in sorafenib resistance in HCC are still lacking.

Whole transcriptome sequencing (WTS) is a one-stop solution that focuses on the aggregation of all transcriptional products (lncRNAs, circRNAs, miRNAs and mRNAs) in specific cells or tissues in a certain state. It can be used to conduct multiple RNA joint analyses, internal ceRNA integration analysis, molecular marker screening, and to explore potential regulatory network mechanisms [16]. Here, WTS was exhibited in sorafenib-resistant HCC cell lines Huh7/S and SMMC7721/S compared with their parental cells. In particular, 257 upregulated and 177 downregulated lncRNAs were identified in SMMC7721/S cells compared to those in SMMC7721 cells, and 65 upregulated and 115 downregulated lncRNAs were identified in Huh7/S cells compared to those in Huh7 cells. Alternatively, 61 and 19 upregulated, but 40 and 11 downregulated circRNAs have been determined in SMMC7721/S cells and Huh7/S cells, respectively, compared to Huh7 and SMMC7721 cells. Furthermore, 83 downregulated and 84 upregulated miRNAs in SMMC7721/S cells; 40 downregulated and 41 upregulated miRNAs in Huh7/S cells were screened. Additionally, the overlapped differentially expressed ncRNAs (DENs) in both SMMC7721/S and Huh7/S cells including the lncRNA SNHG1-229, lncRNA MED17-203, lncRNA SPINT1-AS1-202, lncRNA TPM1-233, lncRNA TPM4-229, circ_0001944, circ_0078607, circ_0002874, miR-193a-5p, miR-197-3p, miR-27a-5p, miR-320b, miR-767-3p, miR-767-5p, miR-92a-3p and let-7c-5p were identified for the first time in sorafenib-resistant HCC.

Accordingly, the three networks firstly stood head and shoulders, where the overlapping DENs and their target genes in both SMMC7721/S and Huh7/S cells may be interrelated to promote sorafenib resistance in HCC. In particular, the network "lncRNA MED17-203-miRNA (miR-193a-5p, miR-197-3p, miR-27a-5p, miR-320b, miR-767-3p, miR-767-5p, miR-92a-3p, let-7c-5p)-mRNA" was involved in the lipid and alpha-amino acid metabolic, as well as the fatty acid transport process, and was enriched in the PPAR and HIF-1 signaling pathways. Alternatively, the network "circ_0002874-miR-27a-5p-mRNA" participated in the alpha-amino acid metabolic, cell-cell adhesion and ion transport process, as well as the activation of the Hippo signaling pathway. Furthermore, the network "circ_0078607-miR-320b-mRNA" was enriched in vesicle-mediated transport process, which can be regulated by the activation of the TGF-β signaling pathway. These findings suggested that the "lncRNA MED17-203-miRNA-mRNA," "circ_0002874-miR-27a-5p-mRNA," and "circ_0078607-miR-320b-mRNA" networks should not be in the shadows, but can be valued for their roles to promote sorafenib resistance by encouraging metabolic reprogramming where the activation of PPAR, HIF-1, Hippo and TGF-β signaling pathways was regulated. Moreover, the network "circ_0002874-miR-27a-5p-mRNA" may also be widely distributed in Epithelial-mesenchymal transition (EMT), in addition to metabolic reprogramming to encourage sorafenib resistance in which the activation of the Hippo signaling pathway is modulated.

Taken together, these detailed and originality findings point to a new path and direction for exploring the mechanisms inducing sorafenib resistance, and thus searching for reliable means to reverse sorafenib resistance in HCC.

2. Materials and methods

2.1. Cells

SMMC7721 and Huh7 cells were obtained from Cell Bank of the Chinese Academy of Sciences (Shanghai, China). Two sorafenib-resistant HCC lines SMMC7721/S and Huh7/S, were established *in vitro* using the continuity induction method. Briefly, SMMC7721 and Huh7 cells at the logarithmic growth phase were seeded in the culture medium containing sorafenib at an initial concentration of 1 μmol/L. Every two days later, surviving cells were re-collected and cultured with a fresh medium having a higher concentration of sorafenib (increasing by 0.1 μmol/L each time). The construction of SMMC7721/S and Huh7/S cells was completed over 8 months.

2.2. RNA quantification and qualification

The SMMC7721, Huh7, SMMC7721/S, and Huh7/S cells were collected. Total RNA was extracted using a TRIZOL reagent. RNA degradation and contamination were monitored using 1 % agarose gel electrophoresis. The RNA purity was assessed using a Nano-Photometer® spectrophotometer (IMPLEN, CA, USA). RNA concentration was measured using Qubit® RNA Assay Kit in Qubit® 2.0 Fluorometer (Life Technologies, CA, USA). RNA integrity was assessed using the RNA Nano 6000 Assay Kit on a Bioanalyzer 2100 system (Agilent Technologies, CA, USA).

2.3. Library preparation for transcriptome sequencing

A total amount of 3 μg RNA per sample was used as input material for the RNA sample preparations. Sequencing libraries were generated using NEBNext® UltraTM RNA Library Prep Kit for Illumina® (NEB, USA) following manufacturer's recommendations, and index codes were added to attribute sequences to each sample. Briefly, mRNA was purified from the total RNA using poly T oligo-attached magnetic beads. Fragmentation was carried out using divalent cations at elevated temperature in the NEBNext First Strand Synthesis Reaction Buffer. The first strand cDNA was synthesized using random hexamer primers and M-MuLV Reverse Transcriptase. Second strand cDNA synthesis was subsequently performed using DNA polymerase I and RNase H. The remaining overhangs were converted into blunt ends via exonuclease/polymerase activity. After adenylation of 3′ ends of DNA fragments, NEBNext Adaptor with hairpin loop structure was ligated to prepare for hybridization. To select cDNA fragments of preferentially 150–200 bp in length, the library fragments were purified using the AMPure XP system (Beckman Coulter, Beverly, USA). Then, 3 μL USER Enzyme (NEB, USA) was used with size-selected, adaptor-ligated cDNA at 37 °C for 15 min followed by 5 min at 95 °C before PCR. PCR was performed using the Phusion High-Fidelity DNA polymerase, Universal PCR primers, and Index (X) Primer. Finally, PCR products were purified (AMPure XP system), and library quality was assessed using an Agilent Bioanalyzer 2100 system.

2.4. Clustering and sequencing

Qualified libraries were pooled and sequenced on an Illumina platform using the PE150 strategy to analyze differentially expressed lncRNAs and circRNAs. Alternatively, clustering of the index-coded samples was performed on a cBot Cluster Generation System using the TruSeq PE Cluster Kit v3-cBot-HS and SE50 (Illumina) to analyze differentially expressed miRNAs and mRNAs. After cluster generation, the library preparations were sequenced on an Illumina HiSeq platform, and 125 bp/150 bp paired-end reads were generated.

2.5. Reads mapping to the reference genome

Raw data (raw reads) in the FASTQ format were first processed using in-house Perl scripts. In this step, clean data (clean reads) were obtained by removing following reads: (1) reads with 5′ adapter; (2) reads without 3′ adapter or insert sequence; (3) reads with more than 10 % N; (4) reads with more than 50 % nucleotides with Qphred $\leq$ 20; (5) reads with ploy A/T/G/C. Adapter trimming for the removal of adapter sequences from the 3' ends of reads was also performed. Simultaneously, Q20, Q30, and GC contents of the clean data were calculated. All downstream analyses were based on clean, high-quality data. The reference genome and gene model annotation files were downloaded directly from the genome website. The index of the reference genome was built using STAR [17] or HISAT2 (V2.0.5) [18] software, and clean paired-end clean reads were aligned to the reference genome using HISAT2 (V2.0.5) or STAR (V2.5.1b) software. In particular, clean reads for each sample were first mapped to a reference genome using the software HISAT2. STAR uses the maximal applicable prefix (MMP) method, which can generate precise mapping results for junction reads. The small RNA tags were also mapped to reference sequence using the Bowtie-0.12.9 software [19] to process raw sequencing data to get the reads count of miRNA.

2.6. Identification of ncRNAs and mRNAs

The read alignment results for lncRNAs were transferred to the StringTie program (StringTie1.3.3b) for transcript assembly. All the transcripts were merged using Cuffmerge software. LncRNAs and mRNAs were then identified from the assembled transcripts following four steps: (1) Removal of lowly expressed transcripts with Fragments Per Kilobase of transcript sequence per Millions base pairs sequenced (FPKM)<0.5; (2) Removal of short transcripts<200 bp and <2 exons; (3) Removal of the transcripts mapped within the 1 kb flanking regions of an annotated gene using Cuffcompare software. In particular, the transcripts with protein-coding capability using CNCI, Pfam and CPC2 database were identified as the predicted mRNAs. LncRNAs were distinguished from mRNAs by comparing the transcript length, exon count, and ORF length. Novel lncRNAs were named following rules of The HUGO Gene Nomenclature Committee (HGNC). The characteristics of novel lncRNA was compared with known lncRNA and mRNA. Alternatively, the circRNAs were detected and identified using *find_ circ* [20] and *CIRI2* [21]. Circos software was used to construct the circos figure. Furthermore, mapped small RNA tags were used to looking for known miRNA. MiRBase20.0 was used as reference, modified software mirdeep2 [22] and srna-tools-cli were used to obtain the potential miRNA and draw the secondary structures. The available software miREvo [23] and mirdeep2 were integrated to predict novel miRNA through exploring the secondary structure. Custom scripts were used to obtain the miRNA counts as well as base bias on the first position of identified miRNA with certain length and on each position of all identified miRNA respectively.

2.7. Quantification of gene expression level

When the quantification of expression level of circRNA and miRNA was performed, the raw counts were first normalized using transcript per million (TPM) through the following criteria: Normalized expression level = ReadCount*1,000,000)/libsize (libsize is the sum of circRNA or miRNA readcount). Alternatively, quantification of lncRNA and mRNA was identified following two steps: (1) The read numbers mapped to each gene were counted using the HTSeq (V0.6.0); (2) Reads Per Kilobase of transcript per Million mapped reads (RPKM) were obtained. The FPKM of each gene was calculated based on the length of the gene and the read count mapped to the gene. FPKM, the expected number of Fragments Per Kilobase of transcript sequence per million base pairs sequenced, considers the effect of sequencing depth and gene length on the read count simultaneously and is currently the most commonly used method for estimating gene expression levels.

2.8. Differential expression analysis

The GATK (V4.1.1.0) software was used to perform SNP calling. Raw VCF files were filtered using the GATK standard filter method and other parameters (cluster:3, WindowSize:35, QD < 2.0, FS > 30.0, and DP < 10). The read counts were adjusted by edgeR program package with one scaling normalization factor.

Differential expression analysis of circRNAs and miRNAs was performed using the DESeq2 R package (V1.20.0). Differential expression analysis of lncRNAs and mRNAs was exhibited using Cuffdiff or edgeR (V3.2.4). P-values were adjusted using the Benjamini & Hochberg method for controlling the false discovery rate. Significantly differentially expressed genes were screened based on the following criteria: Corrected P-value<0.05 (Padj<0.05) and an absolute fold change of two was set as the threshold for significantly differential expression. In particular, overlapping DENs in SMMC7721/S and Huh7/S cells were identified.

2.9. Identification for the target genes of DENs

LncRNAs share the same transcript with mRNAs and regulate the expression of target genes (mRNAs) through "co-localization" or "co-expression" [24]. Herein, the target mRNAs of the differentially expressed lncRNAs were predicted using the *"co-localization"* and *"co-expression"analysis*. In particular,"co-localization" was considered to be the nearest location based on a reference genome map using reads mapping. "Co-localization-expressed" genes were identified based on the positional relationship between lncRNA and mRNA within a range of 100 kb. Alternatively, "co-expressed" genes were selected based on the correlation between lncRNA and mRNA expression, with screening conditions requiring a *pearson correlation coefficient* greater than 0.95. CircRNAs are found to be produced from pre-mRNA back-splicing of thousands of genes in eukaryotes [25]. Thus, the target mRNAs of the differentially expressed circRNAs were determined as the source genes of circRNAs in the reference genome map Target mRNAs of differentially expressed miRNAs were predicted using intersecting analysis of *miRanda and RNAhybrid* software [26,27]. Finally, the target genes were identified as the overlaps between the predicted genes of these DENs and differentially expressed mRNAs obtained using the WTS analysis.

2.10. Interaction correlation analysis between DENs and mRNAs

Intersection analysis between target genes of overlapping lncRNAs and miRNAs in both SMMC7721/S and Huh7/S cells was performed. Intersection analysis between target genes of overlapping circRNAs and miRNAs in both SMMC7721/S and Huh7/S cells was also exhibited. According to ceRNA theory, there is a competitive relationship between miRNAs that interact with lncRNAs or circRNAs. The "lncRNA -miRNA-mRNA" network was constructed based on ceRNA theory using the Cytoscape software where overlapped mRNAs of lncRNAs and miRNAs, as well as overlapping DENs in both SMMC7721/S and Huh7/S cells were involved in. The "circRNA-miRNA-mRNA" network was also constructed in which overlapped mRNAs of circRNAs and miRNAs, as well as overlapping DENs in both SMMC7721/S and Huh7/S cells were also involved. In particular, upregulated miRNAs and downregulated lncRNAs or circRNAs and mRNAs, as well as downregulated miRNAs and upregulated lncRNAs or circRNAs and mRNAs, were demonstrated in these networks. The distance and position of ncRNAs in these networks depend on the strength of their expression correlation.

2.11. GO and KEGG enrichment analysis

Gene Ontology (GO) enrichment analysis for the target genes of DENs was implemented using the clusterProfiler R package, in which gene length bias was corrected. GO terms with corrected P-values less than 0.05 were considered significantly enriched by differentially expressed genes. In particular, the GO covers three domains: cellular components (CC), molecular functions (MF), and biological processes (BP).

In living organisms, different genes coordinate with each other to perform their biological functions, and significant enrichment can determine the main biochemical metabolic, and signal transduction pathways in which candidate target genes participate [28].

Kyoto Encyclopedia of Genes and Genomes (KEGG) is a database resource for understanding high-level functions and utilities of the biological systems, such as cells, organisms, and ecosystems, from molecular-level information, especially large-scale molecular datasets generated by genome sequencing and other high-through put experimental technologies (http://www.genome.jp/kegg/) [29] Pathway significance enrichment analysis uses KEGG Pathways as a unit and applies hypergeometric tests to identify pathways that are

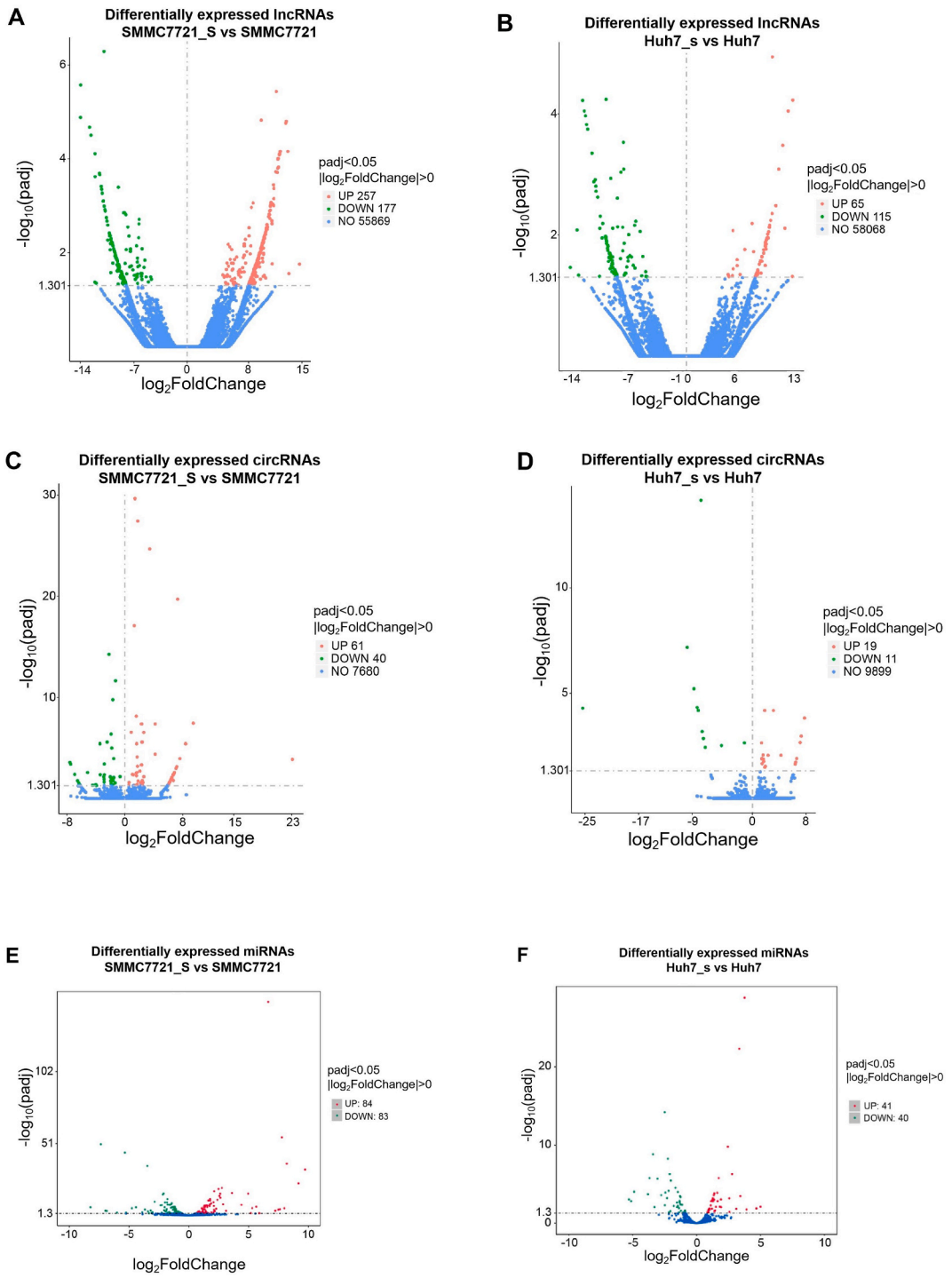

Fig. 1. The determination for DENs in sorafenib-resistant cells, compared to sorafenib-sensitive HCC cells. (A and B) The volcano map for differentially expressed lncRNAs in SMMC7721/S and Huh7/S cells, compared to SMMC7721 and Huh7 cells, respectively. **(C and D)** The volcano plot image for differentially expressed circRNAs in SMMC7721/S compared to SMMC7721 cells **(C)**, and in Huh7/S compared to Huh7 cells **(D). (E and F)** The volcano map for differentially expressed miRNAs in SMMC7721/S, compared to SMMC7721 cells **(E)**, and in Huh7/S, compared to Huh7 cells **(F)**. For the volcano plot image, the horizontal axis represents the change in the expression fold (log2FoldChange) of DENs in different experimental groups/samples, while the vertical axis represents the statistical significance of the change in the expression of DENs. The "UP" and "DOWN" represents the upregulated and downregulated DENs, respectively. Padj is the value obtained using Benjamini and Hochberg's method to perform multiple tests. Padj$<$0.05. Fold Change$\geq$1.0.

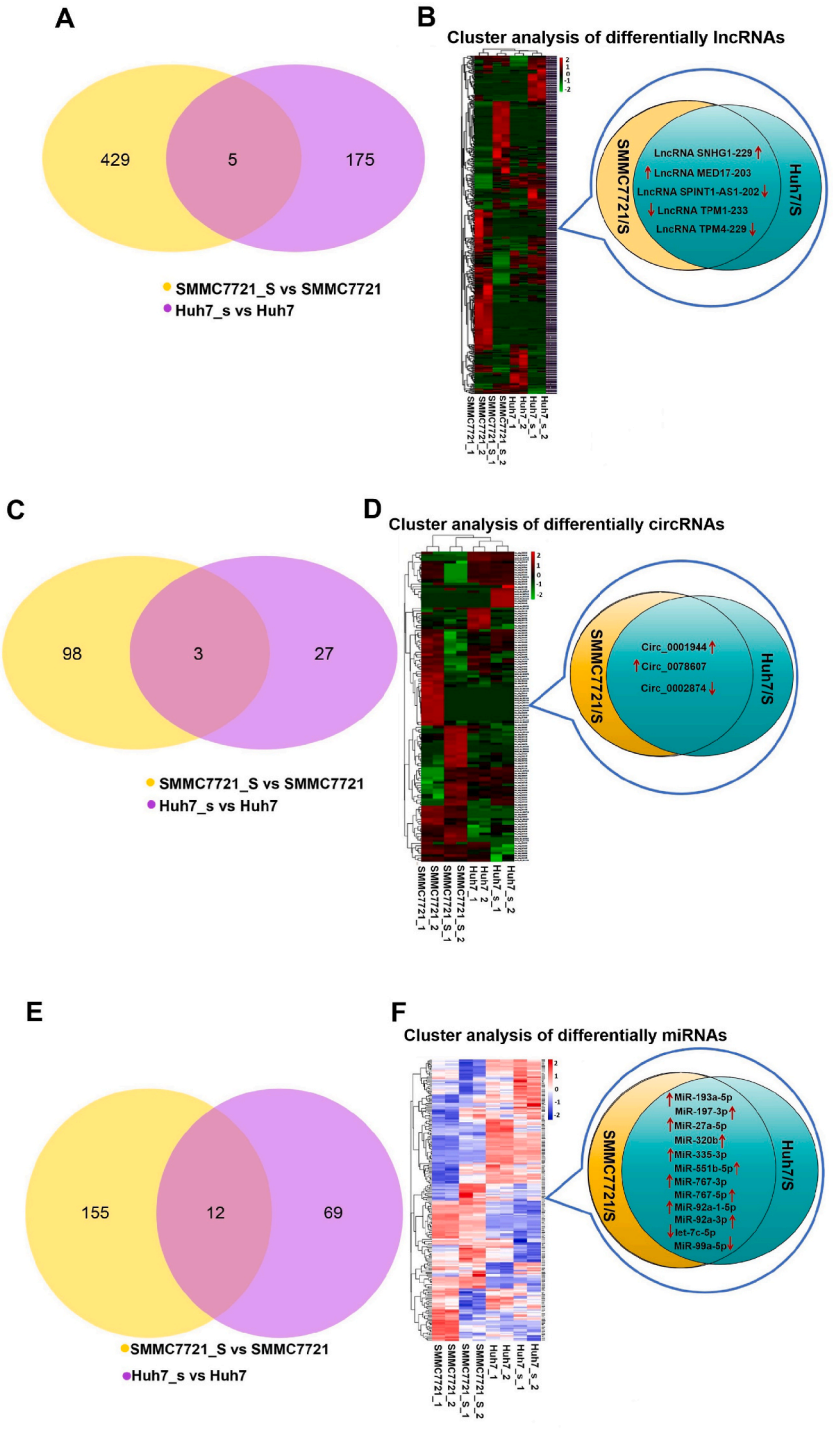

Fig. 2. The identification for DENs, which partially play a vital role in the development of sorafenib resistance. **(A)** The Venn diagram showing the differentially expressed lncRNAs in both SMMC7721/S and Huh7/S cells, compared to their parental cells. **(B)** Details for these differentially expressed lncRNAs in both SMMC7721/S and Huh7/S cells, compared to SMMC7721 and Huh7 cells, respectively. **(C and D)** The Venn map **(C)** and the detail information **(D)** for the differentially expressed circRNAs in both SMMC7721/S and Huh7/S cells, compared to SMMC7721 and Huh7 cells respectively. **(E and F)** The Venn map **(E)** and the details **(F)** for the differentially expressed miRNAs in both SMMC7721/S and Huh7/S cells. The values in the intersection in the Venn map represent the number of DENs in both SMMC7721/S and Huh7/S cells.

significantly enriched in candidate target genes compared to the entire genome background. The R clusterProfiler package was used to test the statistical enrichment of expression genes in the KEGG pathways. The 20 most significant GO and KEGG enrichment pathways are drawn as a bar chart; the horizontal axis in the figure represents the KEGG pathway, and the vertical axis represents the significance level of pathway enrichment, with higher values indicating greater significance.

3. Results

3.1. The identification of DENs in sorafenib-resistant HCC cells

Whole transcriptome sequencing in sorafenib-resistant compared to sorafenib-sensitive HCC cell lines may be used to understand how acquired drug resistance occurs. Therefore, the DENs with fold change≥1 were firstly identified in SMMC7721/S cells and Huh7/S cells, compared to Huh7 and SMMC7721 cells. A total of 257 upregulated and 177 downregulated lncRNAs were identified in SMMC7721/S cells compared to those in SMMC7721 cells (Fig. 1A). In addition, 65 upregulated and 115 downregulated lncRNAs were confirmed in Huh7/S cells compared to Huh7 cells (Fig. 1B). Alternatively, 61 upregulated and 40 downregulated circRNAs were

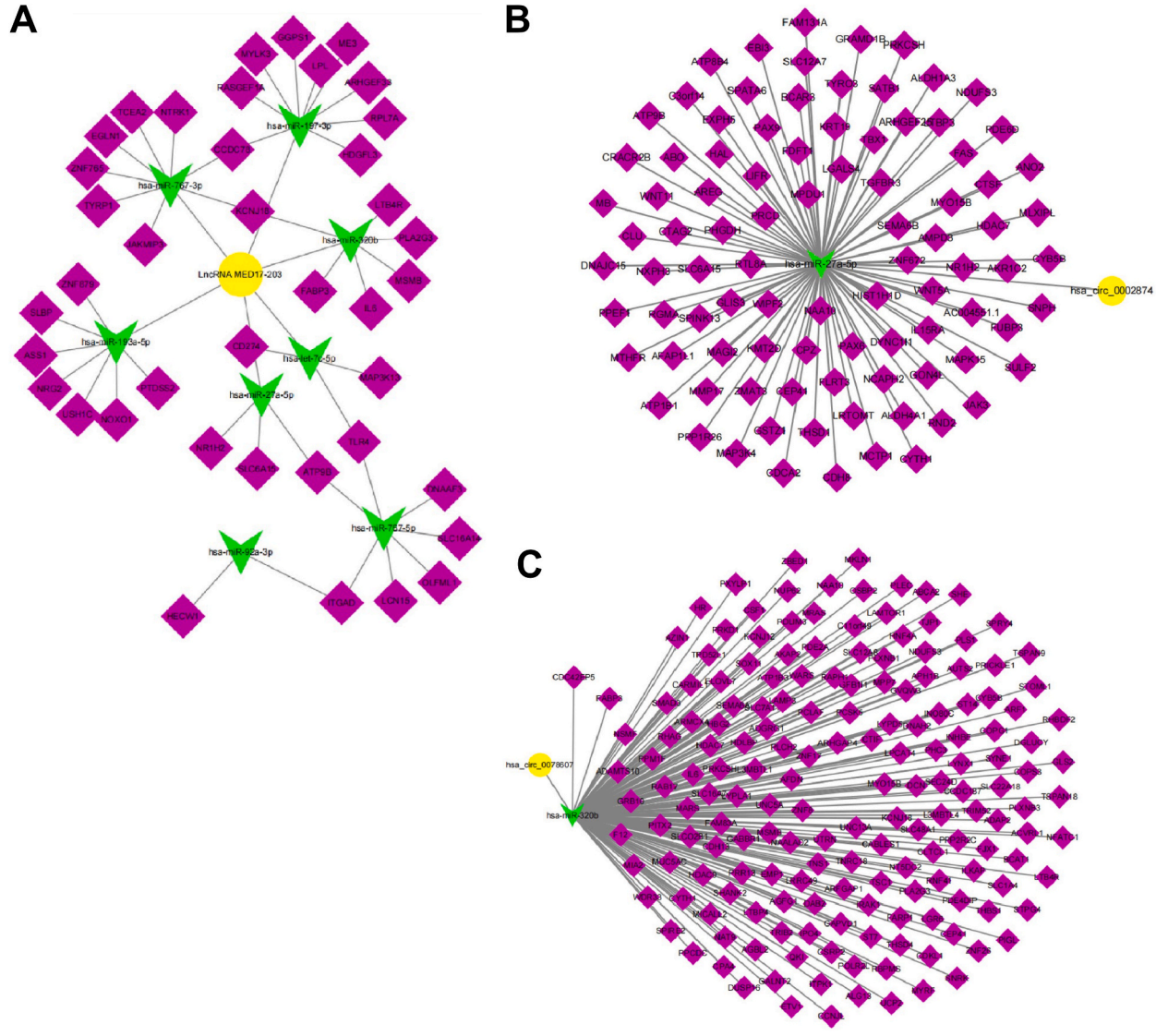

Fig. 3. The construction of an interactive network in sorafenib-resistant HCC cells based on ceRNA theory using the Cytoscape software. **(A)** A network "lncRNA MED17-203-miRNA-mRNA" based on lncRNA MED17-203, miR-193a-5p, miR-197-3p, miR-27a-5p, miR-320b, miR-767-3p, miR-767-5p, miR-92a-3p, let-7c-5p and indicated mRNAs.**(B)** An interactive network "circ_0002874-miR-27a-5p-mRNA" depicts that circ_0002874 targeted miR-27a-5p and downstream mRNAs. **(C)** "Circ_0078607-miR-320b-mRNA" network showing the interactive relationship between circ_0078607, miR-320b, and mRNAs.

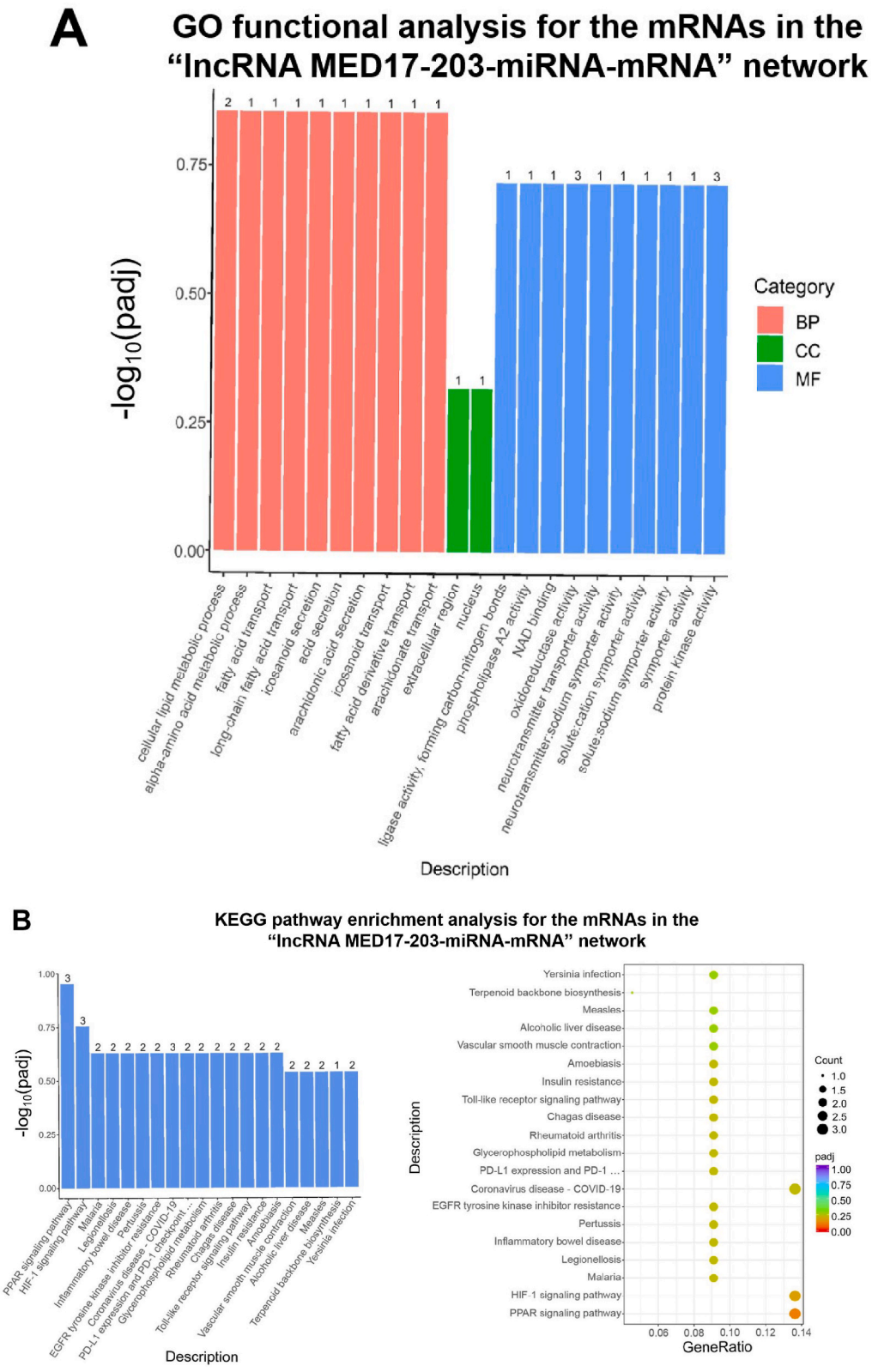

Fig. 4. GO functional and KEGG pathway enrichment analysis for the target genes in these networks. (A) and (B) The enrichment map of GO terms **(A)** and KEGG pathways **(B)** for indicated mRNAs in the "lncRNA MED17-203-miRNA-mRNA" network. **(C) and (D)** GO and KEGG bar for these mRNAs of functional **(C)** and KEGG pathway enrichment **(D)** in the "circ_0002874-miR-27a-5p-mRNA" network. **(E) and (F)** The identification

of GO function **(E)** and KEGG pathway enrichment **(F)** for these mRNAs in the "circ_0078607-miR-miR-320b-mRNA" network. The corrected P-value (Padj) < 0.05 was considered significantly enriched by differentially expressed genes. The 20 most significant GO and KEGG enrichment pathways were drawn as a bar chart.

determined in SMMC7721/S cells compared to those in SMMC7721 cells (Fig. 1C). 19 upregulated and 11 downregulated circRNAs were also identified in Huh7/S cells compared to those in Huh7 cells (Fig. 1D). 84 upregulated and 83 downregulated miRNAs in SMMC7721/S cells (Fig. 1E); 41 upregulated and 40 downregulated miRNAs in Huh7/S cells were screened (Fig. 1F). The heatmaps showing the differentially expressed ncRNAs with similar patterns were obtained using the clustering analysis and were shown in Supplementary Fig. 1.These findings point the way for further exploration of the function of differentially expressed ncRNA-related sorafenib resistance in HCC.

3.2. The identification for DENs suspected to sorafenib resistance in HCC cells

As shown in Fig. 1, so many DENs were obtained from the two separate sorafenib-resistant HCC lines; therefore, it was difficult to identify novel markers involved in sorafenib resistance. Interestingly, the target genes of differentially expressed miRNAs in SMMC7721/S and Huh7/S cells were enriched in the processes of protein phosphorylation, intracellular signal transduction and cell-cell adhesion. However, no overlap in gene function and pathway enrichment for the target genes of these differentially expressed lncRNAs or circRNAs in both SMMC7721/S and Huh7/S cells was found (Supplementary Fig. 2). Thus, we focused on DENs with an intersection between SMMC7721/S cells and Huh7/S cells to identify common issues that encourage sorafenib resistance in HCC. In particular, 2 upregulated (lncRNA SNHG1-229 and lncRNA MED17-203) and 3 downregulated lncRNAs (lncRNA SPINT1-AS1-202, lncRNA TPM1-233 and lncRNA TPM4-229) in both SMMC7721/S and Huh7/S cells attracted our attention (Fig. 2A and B). As demonstrated in Fig. 2C and D, 2 upregulated circRNAs (circ_0001944 and circ_0078607) and 1 downregulated circRNA (circ_0002874) in both SMMC7721/S and Huh7/S cells were also of interest. Moreover, 10 upregulated (miR-193a-5p, miR-197-3p, miR-27a-5p, miR-320b, miR-335-3p, miR-551b-5p, miR-767-3p, miR-767-5p, miR-92a-1-5p, and miR-92a-3p) and 2 downregulated miRNAs (let-7c-5p and miR-99a-5p) in both SMMC7721/S and Huh7/S cells were confirmed (Fig. 2E and F).

3.3. The depiction of interactive network diagrams involved in the development of sorafenib resistance in HCC

Based on the findings mentioned above, it is unclear whether an interactive network exists among the DENs with an intersection between these two sorafenib-resistant HCC cells. In particular, the "lncRNA-miRNA-mRNA" network was constructed based on ceRNA theory using the Cytoscape software, where overlapping mRNAs of lncRNAs and miRNAs, as well as DENs in both SMMC7721/S and Huh7/S cells were involved in. The "circRNA-miRNA-mRNA" network was also constructed in which overlapping mRNAs of circRNAs and miRNAs, as well as DENs in both SMMC7721/S and Huh7/S cells were also involved. Herein, a network based on "lncRNA MED17-203-miRNA-mRNA" has been identified in which lncRNA MED17-203, miR-193a-5p, miR-197-3p, miR-27a-5p, miR-320b, miR-767-3p, miR-767-5p, miR-92a-3p, let-7c-5p, and indicated mRNAs were involved (Fig. 3A). Interestingly, KCNJ18 was located at the hub of the network, in which lncRNA MED17-203 targeted miR-197-3p, miR-767-3p, and miR-320b. Furthermore, a network "circ_0002874-miR-27a-5p-mRNA" based circ_0002874 and miR-27a-5p was also established, as shown in Fig. 3B. PRCD, MPDU1, LGALS4, NAA10, TGFBR3, SEMA6B, ZNF672, HIST1H1D, WIPF2, and RTL8A represented several mRNAs at the forefront of the charge in terms of the interactive relationships between circ_0002874, miR-27a-5p, and the indicated mRNAs. Similarly, another "circRNA-miRNA-mRNA" network was provided, as demonstrated in Fig. 3C. In particular, circ_0078607 targeted miR-320b to regulate downstream gene expression. CDC42EP5, FABP3, NSMF, ADAMTS10, GRB10, F12, IA2, and MIA2 attracted considerable attention in this network because they are closely related to miR-320b.

3.4. The identification for the function and pathway enrichment of the target genes in these networks

These findings prompted us to continue exploring the mechanisms underlying sorafenib resistance, which are clearly related to overlapping DENs and their target genes. Thus, functional and pathway enrichment analysis of the target genes in these networks were performed. GO functional and KEGG pathway enrichment analysis demonstrated that these mRNAs located in the "lncRNA MED17-203-miRNA-mRNA" network were involved in the lipid and alpha-amino acid metabolic, as well as the fatty acid transport process (Fig. 4A and Supplementary Figs. 3A–C). Moreover, these mRNAs based on this network were enriched in the PPAR and HIF-1 signaling pathways (Fig. 4B).

Alternatively, these mRNAs in the "circ_0002874-miR-27a-5p-mRNA" regulatory network were involved in the alpha-amino acid metabolic, cell-cell adhesion, and ion transport process (Fig. 4C and Supplementary Figs. 3D–F). They participated in the activation of the Hippo signaling pathway (Fig. 4D).

Additionally, GO and KEGG pathway analysis for indicated mRNAs involved in the "circ_0078607-miR-320b-mRNA" network was also carried out. These mRNAs were enriched in the vesicle-mediated transport process (Fig. 4E and Supplementary Figs. 3G–I), which can be regulated by the activation of the TGF-β signaling pathway (Fig. 4F).

A steady influx of fatty acids and ions, as well as a well-recognized increase in lipids and amino acids, may comprise an important chapter in the story of metabolic reprogramming [30]. Thus, we can assume that these networks can be considered as a motive force to support sorafenib resistance in HCC by promoting metabolic reprogramming. Alternatively, EMT is recognized as a reversible change in the process of epithelial cells transforming into mesenchymal phenotype cells, where cytoskeletal recombination loses polarity and

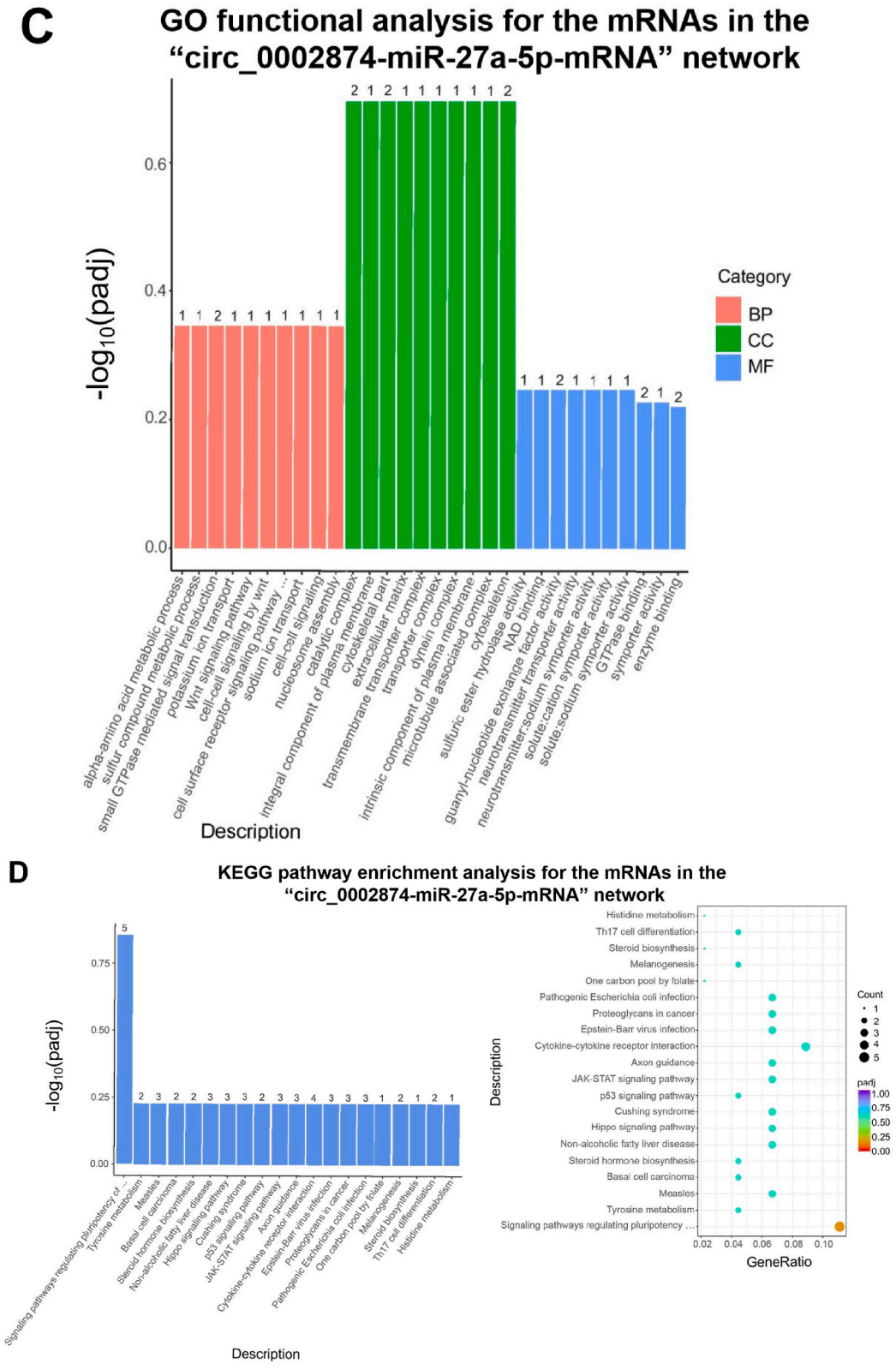

Fig. 4. (*continued*).

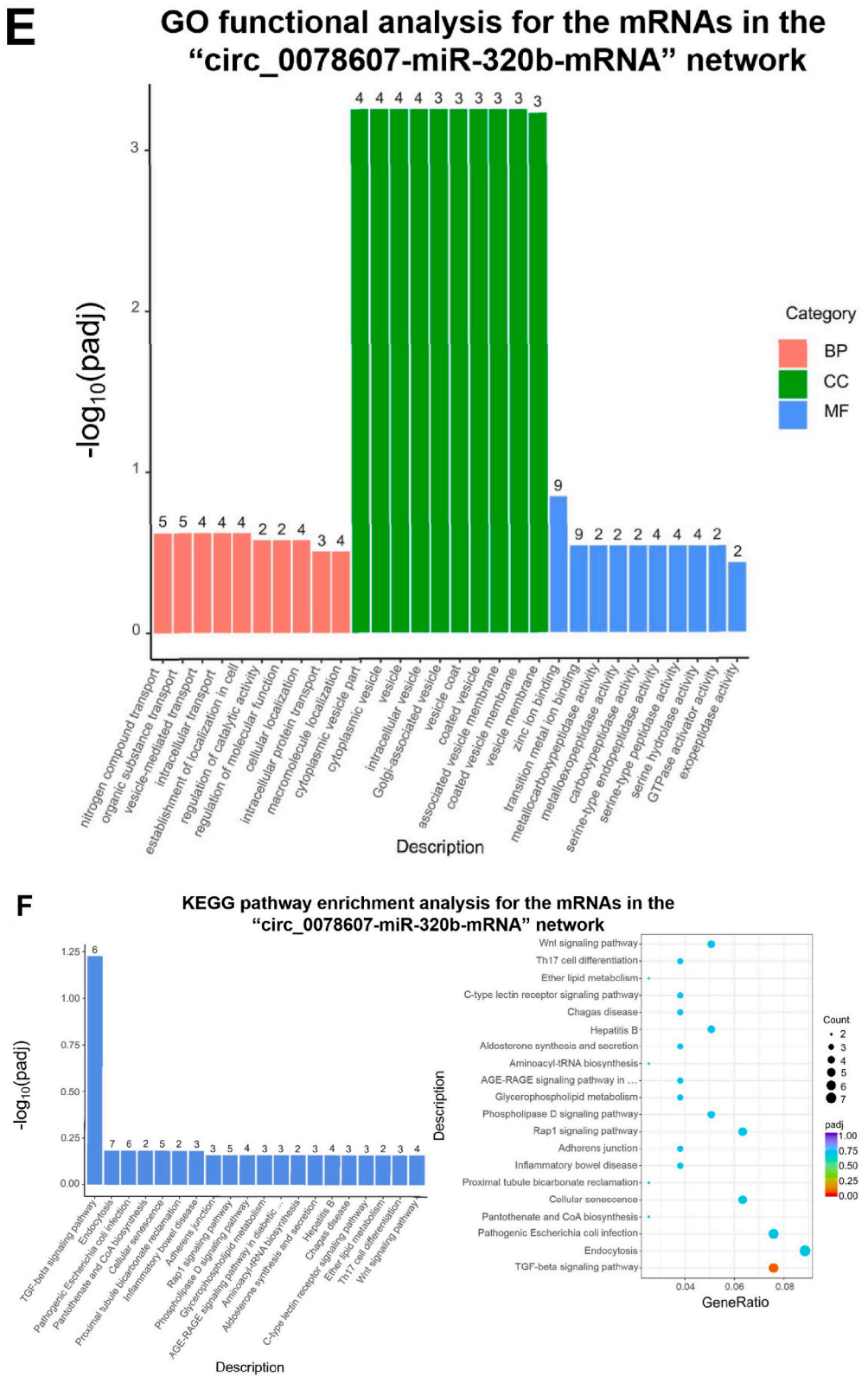

Fig. 4. (*continued*).

adhesion weakens, resulting in increased cell motility and invasiveness, as well as enhanced cell-cell adhesion [31]. It is reasonable to speculate that EMT is another mechanism encouraging aggressive malignant bio-behaviors of sorafenib-treated HCC cells where the network "circ_0002874-miR-27a-5p-mRNA" is also involved in.

4. Discussion

Sorafenib can prolong the survival period and improve the quality of life of patients with advanced HCC, but it has been shown to offer unfavorable outcomes in patients with resistant conditions. The mechanisms underlying sorafenib resistance in HCC are poorly understood.

Traditionally, enhanced DNA repair, altered drug targets, drug inactivation, reduced drug absorption, and increased drug efflux have been the major mechanisms that advance drug resistance in tumor cells [32]. However, tumor cells progressively optimize themselves to accumulate genetic alterations, thus accommodating a complicated TME [33]. These so-called "successful" tumor cells exhibited intratumor heterogeneity and constructed such epigenetic genetic maps, where ncRNAs, including lncRNAs, circRNAs, and miRNAs, played the role of a sentry very well. Some are tipped to trigger drug resistance, whereas others may be fortunate guards, but they are also defeated at the end of in the story of drug resistance [34].

However, previous studies have mostly focused on selecting a type of sorafenib-resistant cell line and analyzing a specific ncRNA, where *Microarray analysis* was usually exhibited. Subsequently, ncRNAs involved in sorafenib resistance in HCC are selected by borrowing their roles in the progress of drug resistance in other types of tumors. Therefore, novel ncRNAs may be dropped out of sight while exploring the mechanisms underlying sorafenib resistance in HCC. Herein, WTS but not Microarray analysis, which was usually used in previous studies, was performed. One-time acquisition of differentially expressed lncRNAs, circRNAs, miRNAs, and mRNAs in sorafenib-resistant HCC cell lines compared to their parental cells was achieved. In particular, the overlap of DENs in both SMMC7721/S and Huh7/S cells derived from different types of parental cells attracted more attention to investigate the mechanisms promoting sorafenib resistance. Interestingly, overlapping DENs, including the lncRNA SNHG1-229, lncRNA MED17-203, lncRNA SPINT1-AS1-202, lncRNA TPM1-233, and lncRNA TPM4-229; circ_0001944, circ_0002874, and circ_0078607; and miR-27a-5p and miR-320b, have not been confirmed in HCC, much less for their implications in sorafenib treatment in HCC. Alternatively,miR-193a-5p [35], miR-197-3p [36], miR-767-3p [37], and let-7c-5p [38] inhibits cell growth, proliferation, and invasion. In contrast, upregulation of miR-767-5p correlates well with disease progression and predicts poor prognosis in patients with HCC [39]. MiR-92a-3p also promotes the malignant progression of HCC by mediating the PI3K/AKT/mTOR signaling pathway [40]. However, these miRNAs have not been reported to be associated with sorafenib treatment of HCC. Collectively, our findings have identified some novel ncRNAs that may be provided with greater "powers" to encourage sorafenib resistance in HCC.

Obviously, the target genes of these DENs, as well as the interactive network among these target genes and DENs, should be identified to provide more convincing evidence regarding their role in encouraging sorafenib resistance in HCC. Herein, the "lncRNA MED17-203-miRNA-mRNA," "circ_0002874-miR-27a-5p-mRNA" and "circ_0078607-miR-320b-mRNA" networks were established. To the best of our knowledge, this is the first report on these networks in sorafenib-resistant HCC.

Subsequently, the functional and enrichment identification of target genes in these networks must be performed to reveal the underlying mechanisms that promote sorafenib resistance in HCC. Interestingly, target genes in these networks are involved in metabolic reprogramming. The activation of the PPAR and HIF-1, Hippo, and TGF-β signaling pathways is highly likely to be closely related to metabolic reprogramming regulated by these networks. Metabolic reprogramming has enjoyed high exposure and is closely related to drug resistance in tumor cells, including HCC [41]. HCC is recognized as one of the most hypoxic malignancies, and the dizziness caused by HIFs induction contributes to drug resistance in sorafenib-treated HCC [42]. It has been found that HIF-mediated induction of metabolic reprogramming is an important mechanism to hinder significantly the efficacy of sorafenib in HCC [43]. Huh7/S cells showed markedly higher glucose uptake and lactate production, indicating augmented glycolysis. HIF-mediated induction of glucose metabolism contributes to sorafenib resistance in multiple HCC cell lines, including Huh7/S cells [44]. Furthermore, HIF-mediated suppression of mitochondrial metabolism is involved in the development of sorafenib resistance by lowering ROS levels in sorafenib-treated hypoxic HCC [45]. Additionally, phosphoglycerate dehydrogenase (PHGDH), the first committed enzyme in the serine synthesis pathway (SSP), has been regarded as a critical driver for sorafenib resistance by increasing the αKG, serine, and NADPH production [46]. More interestingly, the activation of the HIF-1α/PPAR-γ/PKM2 pathway encourages PKM2-mediated glycolysis to inhibit cell apoptosis [47], and PPARδ reprograms glutamine metabolism, thus in-sensitizing HCC cells to sorafenib [48].

However, it is rarely to be reported for the activation of the Hippo and TGF-β signaling pathways in the metabolic reprogramming that promoted sorafenib resistance in HCC. Recently, miR-494 was found to induce metabolic changes that modulate the response to sorafenib in HCC through G6pc targeting [49]. However, few reports involve a clearer explanation for the role of other ncRNAs in metabolic reprogramming and sorafenib resistance in HCC that was mediated by the activation of the PPAR, HIF-1, Hippo, and TGF-β signaling pathways. Moreover, there was no report regarding that the networks "lncRNA MED17-203-miRNA-mRNA," "circ_0002874-miR-27a-5p-mRNA," and "circ_0078607-miR-320b-mRNA" were involved in the regulation of the activation of the PPAR, HIF-1, Hippo and TGF-β signaling pathways to induce sorafenib resistance in HCC by regulating the process of the metabolism and transport of lipid, α-amino acid, fatty acid and ion.

Our findings also suggest that the target genes in the "circ_0002874-miR-27a-5p-mRNA"network are concerned with EMT, where the activation of the Hippo signaling pathway was monitored. EMT is considered a new mechanism leading to drug resistance because tumor cells exhibiting acquired drug resistance often tended to be interstitially differentiated, whereas tumor cells with inherent interstitial differentiation often exhibit primary drug resistance [50]. Previously, our group has revealed that EMT is closely connected to sorafenib resistance in HCC, with ncRNAs playing integral roles in this process [51]. For example, miR-216a/217 encourages EMT

development by activating the PTEN/PI3K/AKT and SMAD7/TGF-β pathways, thereby introducing sorafenib resistance in HCC [52]. LncRNA SNHG3 [53], lncRNA MALAT1 [54], and lncRNA-POIR [55] activate the miR-128/CD151 and miR-140-5p/Aurora-a axis and sponge miR-182-5p, thus encouraging EMT and sorafenib resistance in HCC. LncRNA MAFG-AS1 also promotes EMT and sorafenib resistance in HCC by targeting the miR-3196/STRN4 axis [56]. In contrast, circMEMO1 targets the miR-106b-5p/TET1/5hmC axis to enhance *TCF21 promoter* methylation, which can hinder EMT and improve the sensitivity of HCC cells [57]. However, no reports mentioned that the activation of the Hippo signaling pathway regulated by the "circ_0002874-miR-27a-5p-mRNA" network contributes to the development of EMT and sorafenib resistance in HCC.

Therefore, our findings replenished and deepened previous achievements, and have a great significance for exploring underlining mechanisms that promote sorafenib resistance in HCC, particularly the role of ncRNAs. Although some novelties draw our attention, it is true that there are still many shortcomings to the article. First, the statistically significant and biologically meaningful findings should be distinguished. A series of experiments such as *CCK-8 assay*, *chimeric algorithm prediction, Co-Immunoprecipitation assay, RNA immunopreciptation and Fluorescence in situ hybridization assay* should be conducted to confirm the specific lncRNA or circRNA and miRNA as well as targeted mRNAs in these networks that encourage sorafenib resistance. We intended to focus on KCNJ18, a 48-kDa potassium channel protein that was previously identified in esophageal squamous cell carcinoma for its role in promoting cell cycle and proliferation [58], which is now confirmed firstly in our study. An in-depth exploration will be performed on the exact role of KCNJ18 in this core position in the network, where lncRNA MED17-203 targets miR-197-3p, miR-767-3p, and miR-320b, especially for its implications in the activation of the PPAR and HIF-1 signaling pathways and metabolic reprogramming. Alternatively, we can expand this foundation for investigation based on PRCD, MPDU1, LGALS4, NAA10, TGFBR3, SEMA6B, ZNF672, HIST1H1D, WIPF2, and RTL8A. Because these targeted genes were followed closely behind circ_0002874/miR-27a-5p, and were rarely to be reported about their roles in the activation of the Hippo signaling pathways, as well as metabolic reprogramming, EMT development, and sorafenib resistance in HCC. Similarly, the mechanisms promoting metabolic reprogramming and sorafenib resistance that was closely associated with the activation of the TGF-β signaling pathway should be determined based on CDC42EP5, FABP3, NSMF, ADAMTS10, GRB10, F12, IA2, and MIA2. Because they were tightly bound and close to circ_0078607/miR-320b. Furthermore, the clinical correlation between these overlapping DENs and sorafenib resistance in HCC requires further exploration. The validation of clinical effects is a necessary path to achieve "clinical reversal" through "theoretical exploration," which still has a long way to go.

In conclusion, our data opens new avenues for the optimization of sorafenib applications. In particular, the "lncRNA MED17-203-miRNA-mRNA," "circ_0002874-miR-27a-5p-mRNA," and "circ_0078607-miR-320b-mRNA" networks were highly likely to promote metabolic reprogramming and EMT, thus highlighting a bright future for overcoming sorafenib resistance in HCC.

Ethics approval

This study did not involve any human samples and was approved by the Ethics Committee of the affiliated hospital of Qingdao University.

Funding statement

This work was supported by the National Natural Science Foundation of China (No.82204433).

Data availability statement

The data used to support the findings of this study are available from the corresponding author upon a reasonable request.

CRediT authorship contribution statement

FanJing Jing: Conceptualization. **YunYan Shi:** Formal analysis, Data curation. **Dong Jiang:** Formal analysis, Data curation. **Xiao Li:** Software, Formal analysis, Data curation. **JiaLin Sun:** Software, Formal analysis, Data curation. **XiaoLei Zhang:** Software, Formal analysis, Data curation. **Qie Guo:** Writing – review & editing, Writing – original draft.

Declaration of competing interest

The authors declare that they have no known competing financial interests or personal relationships that could have appeared to influence the work reported in this paper.

Acknowledgments

The authors would like to thank *Elsevier's Language Editing services* for editing our manuscript.

Appendix A. Supplementary data

Supplementary data to this article can be found online at https://doi.org/10.1016/j.heliyon.2024.e29374.

References

[1] B. Alawyia, C. Constantinou, Hepatocellular carcinoma: a Narrative review on current knowledge and future prospects, Curr. Treat. Options Oncol. 24 (2023) 711–724, https://doi.org/10.1007/s11864-023-01098-9.
[2] Z. Fan, et al., Recent therapeutics in hepatocellular carcinoma, Am. J. Cancer Res. 13 (2023) 261–275.
[3] C. Yang, et al., Evolving therapeutic landscape of advanced hepatocellular carcinoma, Nat. Rev. Gastroenterol. Hepatol. 20 (2023) 203–222, https://doi.org/10.1038/s41575-022-00704-9.
[4] S. Wei, et al., Target immune components to circumvent sorafenib resistance in hepatocellular carcinoma, Biomed. Pharmacother. 163 (2023) 114798, https://doi.org/10.1016/j.biopha.2023.114798.
[5] D.J. Good, Non-coding RNAs in human health and diseases, Genes 14 (2023), https://doi.org/10.3390/genes14071429.
[6] S. Adnane, A. Marino, E. Leucci, LncRNAs in human cancers: signal from noise, Trends Cell Biol. 32 (2022) 565–573, https://doi.org/10.1016/j.tcb.2022.01.006.
[7] S. Verma, B.D. Sahu, M.N. Mugale, Role of lncRNAs in hepatocellular carcinoma, Life Sci. 325 (2023) 121751, https://doi.org/10.1016/j.lfs.2023.121751.
[8] X. Zhao, Y. Zhong, X. Wang, J. Shen, W. An, Advances in circular RNA and its applications, Int. J. Med. Sci. 19 (2022) 975–985, https://doi.org/10.7150/ijms.71840.
[9] L.S. Kristensen, T. Jakobsen, H. Hager, J. Kjems, The emerging roles of circRNAs in cancer and oncology, Nat. Rev. Clin. Oncol. 19 (2022) 188–206, https://doi.org/10.1038/s41571-021-00585-y.
[10] H. Meng, R. Niu, C. Huang, J. Li, Circular RNA as a novel biomarker and therapeutic target for HCC, Cells 11 (2022), https://doi.org/10.3390/cells11121948.
[11] B.S. Simpson, H. Pye, H.C. Whitaker, The oncological relevance of fragile sites in cancer, Commun. Biol. 4 (2021) 567, https://doi.org/10.1038/s42003-021-02020-5.
[12] A. Menon, N. Abd-Aziz, K. Khalid, C.L. Poh, R. Naidu, miRNA: a promising therapeutic target in cancer, Int. J. Mol. Sci. 23 (2022), https://doi.org/10.3390/ijms231911502.
[13] S. Khare, T. Khare, R. Ramanathan, J.A. Ibdah, Hepatocellular carcinoma: the role of MicroRNAs, Biomolecules 12 (2022), https://doi.org/10.3390/biom12050645.
[14] J.J. Chan, Y. Tay, Noncoding RNA:RNA regulatory networks in cancer, Int. J. Mol. Sci. 19 (2018), https://doi.org/10.3390/ijms19051310.
[15] B. Chen, et al., Targeting non-coding RNAs to overcome cancer therapy resistance, Signal Transduct. Targeted Ther. 7 (2022) 121, https://doi.org/10.1038/s41392-022-00975-3.
[16] A.G. Kutikhin, M.Y. Sinitsky, A.E. Yuzhalin, E.A. Velikanova, Whole-transcriptome sequencing: a powerful tool for vascular tissue engineering and endothelial mechanobiology, High Throughput 7 (2018), https://doi.org/10.3390/ht7010005.
[17] A. Dobin, T.R. Gingeras, Mapping RNA-seq reads with STAR, Curr Protoc Bioinformatics 51 (2015) 11.14.11–11.14.19, https://doi.org/10.1002/0471250953.bi1114s51.
[18] D. Kim, B. Langmead, S.L. Salzberg, HISAT: a fast spliced aligner with low memory requirements, Nat. Methods 12 (2015) 357–360, https://doi.org/10.1038/nmeth.3317.
[19] B. Langmead, C. Trapnell, M. Pop, S.L. Salzberg, Ultrafast and memory-efficient alignment of short DNA sequences to the human genome, Genome Biol. 10 (2009) R25, https://doi.org/10.1186/gb-2009-10-3-r25.
[20] S. Memczak, et al., Circular RNAs are a large class of animal RNAs with regulatory potency, Nature 495 (2013) 333–338, https://doi.org/10.1038/nature11928.
[21] Y. Gao, J. Zhang, F. Zhao, Circular RNA identification based on multiple seed matching, Briefings Bioinf. 19 (2018) 803–810, https://doi.org/10.1093/bib/bbx014.
[22] M.R. Friedländer, S.D. Mackowiak, N. Li, W. Chen, N. Rajewsky, miRDeep2 accurately identifies known and hundreds of novel microRNA genes in seven animal clades, Nucleic Acids Res. 40 (2012) 37–52, https://doi.org/10.1093/nar/gkr688.
[23] M. Wen, Y. Shen, S. Shi, T. Tang, miREvo: an integrative microRNA evolutionary analysis platform for next-generation sequencing experiments, BMC Bioinf. 13 (2012) 140, https://doi.org/10.1186/1471-2105-13-140.
[24] F. Kopp, J.T. Mendell, Functional classification and experimental dissection of long noncoding RNAs, Cell 172 (2018) 393–407, https://doi.org/10.1016/j.cell.2018.01.011.
[25] L.L. Chen, The biogenesis and emerging roles of circular RNAs, Nat. Rev. Mol. Cell Biol. 17 (2016) 205–211, https://doi.org/10.1038/nrm.2015.32.
[26] J. Krüger, M. Rehmsmeier, RNAhybrid: microRNA target prediction easy, fast and flexible, Nucleic Acids Res. 34 (2006) W451–W454, https://doi.org/10.1093/nar/gkl243.
[27] X. Bo, S. Wang, TargetFinder: a software for antisense oligonucleotide target site selection based on MAST and secondary structures of target mRNA, Bioinformatics 21 (2005) 1401–1402, https://doi.org/10.1093/bioinformatics/bti211.
[28] M. Kanehisa, et al., KEGG for linking genomes to life and the environment, Nucleic Acids Res. 36 (2008) D480–D484, https://doi.org/10.1093/nar/gkm882.
[29] X. Mao, T. Cai, J.G. Olyarchuk, L. Wei, Automated genome annotation and pathway identification using the KEGG Orthology (KO) as a controlled vocabulary, Bioinformatics 21 (2005) 3787–3793, https://doi.org/10.1093/bioinformatics/bti430.
[30] S. Nong, et al., Metabolic reprogramming in cancer: mechanisms and therapeutics, MedComm 4 (2023) e218, https://doi.org/10.1002/mco2.218, 2020.
[31] Z. Xu, Y. Zhang, H. Dai, B. Han, Epithelial-mesenchymal transition-mediated tumor therapeutic resistance, Molecules 27 (2022), https://doi.org/10.3390/molecules27154750.
[32] C. Duan, et al., Overcoming cancer multi-drug resistance (MDR): reasons, mechanisms, nanotherapeutic solutions, and challenges, Biomed. Pharmacother. 162 (2023) 114643, https://doi.org/10.1016/j.biopha.2023.114643.
[33] J. Li, N. Yu, X. Li, M. Cui, Q. Guo, The single-cell sequencing: a dazzling light shining on the dark corner of cancer, Front. Oncol. 11 (2021) 759894, https://doi.org/10.3389/fonc.2021.759894.
[34] L.J. Castro-Muñoz, et al., Modulating epigenetic modifications for cancer therapy, Oncol. Rep. 49 (2023), https://doi.org/10.3892/or.2023.8496 (Review).
[35] J.T. Wang, Z.H. Wang, Role of miR-193a-5p in the proliferation and apoptosis of hepatocellular carcinoma, Eur. Rev. Med. Pharmacol. Sci. 22 (2018) 7233–7239, https://doi.org/10.26355/eurrev_201811_16257.
[36] J.S. Ni, et al., MicroRNA-197-3p acts as a prognostic marker and inhibits cell invasion in hepatocellular carcinoma, Oncol. Lett. 17 (2019) 2317–2327, https://doi.org/10.3892/ol.2018.9848.
[37] M. Wu, J. Deng, D. Yao, S. Li, MiR-767-3p promotes the progression of hepatocellular carcinoma via targeting CASP-3/-9, Am J Transl Res 15 (2023) 2926–2938.
[38] W. Chen, et al., Let-7c-5p down-regulates immune-related CDCA8 to inhibit hepatocellular carcinoma, Funct. Integr. Genomics 23 (2023) 56, https://doi.org/10.1007/s10142-023-00974-9.
[39] L. Zhang, et al., Functional analysis of miR-767-5p during the progression of hepatocellular carcinoma and the clinical relevance of its dysregulation, Histochem. Cell Biol. 154 (2020) 231–243, https://doi.org/10.1007/s00418-020-01878-6.
[40] L. Wang, et al., MiR-92a-3p promotes the malignant progression of hepatocellular carcinoma by mediating the PI3K/AKT/mTOR signaling pathway, Curr. Pharmaceut. Des. 27 (2021) 3244–3250, https://doi.org/10.2174/1381612827666210612054156.
[41] J. Li, X. Li, Q. Guo, Drug resistance in cancers: a free pass for bullying, Cells 11 (2022), https://doi.org/10.3390/cells11213383.
[42] M.H. Bao, C.C. Wong, Hypoxia, metabolic reprogramming, and drug resistance in liver cancer, Cells 10 (2021), https://doi.org/10.3390/cells10071715.
[43] R. Coriat, et al., Sorafenib-induced hepatocellular carcinoma cell death depends on reactive oxygen species production in vitro and in vivo, Mol. Cancer Therapeut. 11 (2012) 2284–2293, https://doi.org/10.1158/1535-7163.Mct-12-0093.
[44] V. Tesori, et al., The multikinase inhibitor Sorafenib enhances glycolysis and synergizes with glycolysis blockade for cancer cell killing, Sci. Rep. 5 (2015) 9149, https://doi.org/10.1038/srep09149.

[45] Y.C. Shen, et al., Activating oxidative phosphorylation by a pyruvate dehydrogenase kinase inhibitor overcomes sorafenib resistance of hepatocellular carcinoma, Br. J. Cancer 108 (2013) 72–81, https://doi.org/10.1038/bjc.2012.559.
[46] L. Wei, et al., Genome-wide CRISPR/Cas9 library screening identified PHGDH as a critical driver for Sorafenib resistance in HCC, Nat. Commun. 10 (2019) 4681, https://doi.org/10.1038/s41467-019-12606-7.
[47] J. Feng, et al., Simvastatin re-sensitizes hepatocellular carcinoma cells to sorafenib by inhibiting HIF-1α/PPAR-γ/PKM2-mediated glycolysis, J. Exp. Clin. Cancer Res. 39 (2020) 24, https://doi.org/10.1186/s13046-020-1528-x.
[48] M.J. Kim, et al., PPARδ reprograms glutamine metabolism in sorafenib-resistant HCC, Mol. Cancer Res. 15 (2017) 1230–1242, https://doi.org/10.1158/1541-7786.Mcr-17-0061.
[49] C. Bergamini, et al., MiR-494 induces metabolic changes through G6pc targeting and modulates sorafenib response in hepatocellular carcinoma, J. Exp. Clin. Cancer Res. 42 (2023) 145, https://doi.org/10.1186/s13046-023-02718-w.
[50] P. Debnath, R.S. Huirem, P. Dutta, S. Palchaudhuri, Epithelial-mesenchymal transition and its transcription factors, Biosci. Rep. 42 (2022), https://doi.org/10.1042/bsr20211754.
[51] F. Jing, X. Li, H. Jiang, J. Sun, Q. Guo, Combating drug resistance in hepatocellular carcinoma: No awareness today, no action tomorrow, Biomed. Pharmacother. 167 (2023) 115561, https://doi.org/10.1016/j.biopha.2023.115561.
[52] H. Xia, L.L. Ooi, K.M. Hui, MicroRNA-216a/217-induced epithelial-mesenchymal transition targets PTEN and SMAD7 to promote drug resistance and recurrence of liver cancer, Hepatology 58 (2013) 629–641, https://doi.org/10.1002/hep.26369.
[53] P.F. Zhang, et al., LncRNA SNHG3 induces EMT and sorafenib resistance by modulating the miR-128/CD151 pathway in hepatocellular carcinoma, J. Cell. Physiol. 234 (2019) 2788–2794, https://doi.org/10.1002/jcp.27095.
[54] L. Fan, et al., Long noncoding RNA MALAT1 contributes to sorafenib resistance by targeting miR-140-5p/aurora-A signaling in hepatocellular carcinoma, Mol. Cancer Therapeut. 19 (2020) 1197–1209, https://doi.org/10.1158/1535-7163.Mct-19-0203.
[55] B.W. Chen, et al., lncRNA-POIR promotes epithelial-mesenchymal transition and suppresses sorafenib sensitivity simultaneously in hepatocellular carcinoma by sponging miR-182-5p, J. Cell. Biochem. 122 (2021) 130–142, https://doi.org/10.1002/jcb.29844.
[56] T. Chen, B. Huang, Y. Pan, Long non-coding RNA MAFG-AS1 promotes cell proliferation, migration, and EMT by miR-3196/STRN4 in drug-resistant cells of liver cancer, Front. Cell Dev. Biol. 9 (2021) 688603, https://doi.org/10.3389/fcell.2021.688603.
[57] Z.R. Dong, et al., CircMEMO1 modulates the promoter methylation and expression of TCF21 to regulate hepatocellular carcinoma progression and sorafenib treatment sensitivity, Mol. Cancer 20 (2021) 75, https://doi.org/10.1186/s12943-021-01361-3.
[58] N. Khalilipour, et al., Familial Esophageal Squamous Cell Carcinoma with damaging rare/germline mutations in KCNJ12/KCNJ18 and GPRIN2 genes, Cancer Genet 221 (2018) 46–52, https://doi.org/10.1016/j.cancergen.2017.11.011.